Results of Using a Wireless Inertial Measuring System to Quantify Gait Motions in Control Subjects

Iris Tien, Steven D. Glaser, Ruzena Bajcsy, *Fellow, IEEE*, Douglas S. Goodin, and Michael J. Aminoff

***Abstract*—Gait analysis is important for the diagnosis of many neurological diseases such as Parkinson's. The discovery and interpretation of minor gait abnormalities can aid in early diagnosis. We have used an inertial measuring system mounted on the subject's foot to provide numerical measures of a subject's gait (3-D displacements and rotations), thereby creating an automated tool intended to facilitate diagnosis and enable quantitative prognostication of various neurological disorders in which gait is disturbed. This paper describes the process used for ensuring that these inertial measurement units yield accurate and reliable displacement and rotation data, and for validating the preciseness and robustness of the gait-deconstruction algorithms. It also presents initial results from control subjects, focusing on understanding the data recorded by the shoe-mounted sensor to quantify relevant gait-related motions.**

***Index Terms*—Ambulatory measurements, gait analysis, inertial sensing, Parkinson's disease, physical activity monitoring, wireless sensing.**

I. Introduction

THERE is no objective test to confirm the early diagnosis of Parkinson's disease. Instead, patients rely on the judgment of skilled clinicians. Indeed, many neurological diseases are diagnosed by clinical observation of the movements, and in particular, the gait, of patients. Specific characteristics of gait, such as truncal flexion, freezing, ignition characteristics, and stride length, are important in this regard. The diagnostic process is thus highly subjective, based on the physician's clinical experience and familiarity with the disease rather than on quantifiable measures. This leaves the diagnosis susceptible to the bias of individual clinicians, variability among clinicians based on disparate experiences, and even diagnostic error. Parkinson's disease currently affects roughly 1.5 million Americans, with an estimated 60 000 new cases diagnosed each year. The higher prevalence of the disease among the elderly (85% of sufferers are over the age of 50) means that there will be increased opportunities for aiding the diagnostic process in the coming years as the population ages.

We have devised a system that provides an objective analysis of gait that will allow clinicians to easily visualize the body movements of walking patients. The inertial measuring system provides numerical estimates for the parameters defining gait, including 3-D absolute displacement and angular displacement values, attitude, and heading, which can be understood in a physically based model. We intend to use this system to characterize the gait of patients with various neurological disorders in order to facilitate their diagnosis. This system will become a natural component of the telemedical infrastructure, in particular, the one currently being implemented in California.

Manuscript received September 8, 2008; revised November 25, 2008; accepted April 14, 2009. Date of publication May 5, 2009; date of current version July 9, 2010. This work was supported in part by the Center for Information Technology Research in the Interest of Society (CITRIS) Seed Grant Program under Grant #22.

I. Tien is with the Center for Information Technology Research in the Interest of Society (CITRIS), University of California, Berkeley, CA 94720 USA (e-mail: itien08@berkeley.edu).

S. D. Glaser is with the Center for Information Technology Research in the Interest of Society (CITRIS), University of California, Berkeley, CA 94720 USA, and also with Intel Berkeley Laboratory, Berkeley, CA 94704 USA. He is also with the Energy Resources Department, Lawrence Berkeley National Laboratory, Berkeley, CA 94720 USA (e-mail: glaser@berkeley.edu).

R. Bajcsy is with the Electrical Engineering and Computer Sciences Department, University of California, Berkeley, CA 94720 USA (e-mail: bajcsy@eecs.berkeley.edu).

D. S. Goodin and M. J. Aminoff are with the Neurology Department, University of California, San Francisco, CA 94143 USA (e-mail: douglas.goodin@ucsf.edu; aminoffm@neurology.ucsf.edu).

Color versions of one or more of the figures in this paper are available online at http://ieeexplore.ieee.org.

Digital Object Identifier 10.1109/TITB.2009.2021650

II. Related Work and Background

A. Hardware

In the past, studies of gait in patients with neurological disorders were performed using clinical stride analyzers that consist of force-sensitive insoles placed in the patient's shoes, with data sent to some collection apparatus attached to the patient [1]–[4], special gait analysis devices [5], or video capture [6]. All of these methods were limited to deployment in clinical settings. The insoles are limited to the collection of data from subjects walking down hallways no more than 10–12 m in length [2]–[4]. The data-collection apparatus (an ankle-worn recorder [1] or backpack [3]) are cumbersome enough to interfere with patient movement. Special gait analysis devices can be complicated and difficult to operate, such as using threads that connect to a pulley, which is then connected to an optical length–voltage transducer [5]. Video capture methods are limited to a fixed motion laboratory location, use multiple cameras (six in [6]), and require precise and involved calibration using a network of wands and markers (15 in [6]) before data collection. An alternative to the insoles has been pressure-sensitive piezoelectric floor sensors that are laid out like tiles along hospital corridors [7]. This again poses limitations as data can be collected only over a relatively short distance and only on flat terrain in a constrained area. Moreover, many aspects of gait (e.g., posture, coordination of body parts, etc.) are not captured by such a system. Rather than tiles, some studies have involved force platforms mounted on a walkway with photocells on either side to measure walking speed [8]. However, with this method, trials where the subjects contact the force platforms improperly must be rejected from the analyses, and the length of two platforms, as used in [8],

allows only two consecutive steps on the force platforms to be measured.

Our inertial measurement units are simple and relatively inexpensive, providing a clear clinical cost benefit, ease of use, and infrastructural advantage over current gait-monitoring systems. The units attached to the body are small and light enough to have minimal interference with subject movements. With the sensor attached, subjects are able to walk as they normally would without the sensors, and the movements measured by the sensors accurately reflect multiple aspects of the patient's natural movements.

Our system further addresses the limitations of current methods by being able to collect data over long distances, with the battery life (hours to days) as the limiting factor. The wireless nature of the system allows data to be collected far beyond the limits of a hallway, for example, up or down stairs, and uphill and downhill. Data can also be collected in the home or other locations that reflect the daily routine of patients for the most accurate and useful data acquisition, rather than in artificial clinical settings, where many patients may feel uncomfortable and may therefore not behave naturally. All these data are available to the clinician no matter how distant the patient is; the possibilities of telemedicine may allow assessment by experts at a distance.

The new science of our project currently resides in the measurement domain:

1) Traditional pattern recognition uses very unintuitive classifiers based on acceleration. By converting acceleration into displacement, clinicians are provided with numerical measures that are physical analogs, and it is these physical measures that will be used in attempts to discriminate between healthy subjects and patients with neurological disorders.
2) Providing a more detailed and broader range of gait parameters: Full recording of all foot motions in 6-DOF over 10 ms time steps means that even slight nuances of body movement are captured. The system can lead to sophisticated gait analysis to provide quantified numerical measures of gait far beyond those of cadence and stride length, including but not limited to: the rotation of the foot along the three axes during a step, horizontal and vertical displacement of the foot during a step, and utilizing data from two sensors, asymmetry between the left and right feet.

B. Data Analysis

The previous studies using traditional methods have been primarily concerned with two basic parameters of gait due to technical limitations: cadence (steps per minute) and stride length. Parkinsonian patients exhibit marked gait hypokinesia, or abnormally diminished muscular function or mobility, specifically with regards to regulating stride length to adapt to characteristics of their surroundings or objects in their external environment [3]. To compensate, studies have found that Parkinsonian patients demonstrate an increased cadence and decreased stride length compared to the gait of control subjects [2]. Studies have also found that patients with Parkinson's disease have a decreased ability to maintain a steady gait, with the stride-to-stride variability in gait cycle timing and in the subphases of the gait cycle increased in Parkinsonian patients compared to controls, and a correlation between the degree of gait variability and disease severity [1]. The result is that a Parkinsonian patient's gait is less smooth than in non-Parkinsonian subjects, and is characterized by short and shuffling steps. In patients with multiple sclerosis, studies have found that those with the disease walk slowly, with reduced stride length and cadence, and increased gait variability [4], [9].

More recent work using inertial sensing systems to evaluate gait [10]–[12] have continued to focus on the parameters of cadence and stride length. The inertial measurement units in [12] measured stride length, walking speed, and incline, and reconstructed the sagittal trajectory of a sensed point on the instep of the foot. Their method of data analysis assumed that the sensors were located exactly along the axes in the sagittal plane and that the leg was limited to planar motion. The shoe-mounted sensor package in [11] measured stride length and stride velocity, breaking up the temporal variable of velocity into heel strike timing and toe-off timing.

Analysis of the data collected by our inertial measuring system allows for a 3-D reconstruction of foot flight during walking, beyond just the sagittal trajectory, and without assuming planar leg motion, a clear advantage over previous studies [12]. Our sensor does not need to be located exactly along the axes of the sagittal plane as was necessary with others [12], since we use gravity measurements to correct for the orientation of the sensor on the foot. The sensor on the foot in our system acquires a broader and more detailed range of measurements about a person's gait, including continual 6-DOF monitoring of the movement of the foot through the air for each step. This allows numerical data to be obtained not just of heel strike and toe lift-off (e.g. [11]), but of all the foot's motions. The raw data from the accelerometers and gyroscopes in the sensor package as displayed in most existing studies ([10], [13]–[17]), cannot be easily understood in physical terms by clinicians or others. In our data analysis, we convert the data from the accelerometers and gyroscopes into 3-D absolute displacement and angular displacement values, which are physical measures that are more meaningful to clinicians.

III. Method

A. Hardware

Our inertial measuring system utilizes commercially available sensor units. Current experiments use MicroAHRS custom units built out of the commercial-off-the-shelf (COTS) wireless, 3DM-GX2 model Gyro Enhanced Orientation Sensor manufactured by MicroStrain, Inc. [18]. The device is 41 mm $\times$ 63 mm $\times$ 32 mm in size and weighs 39 g, and includes a 50-g triaxial accelerometer, 1200°/s triaxial rate gyroscope, and a 2-Gauss triaxial magnetometer. For each unit, each DOF is calibrated to military specifications at the factory before delivery [19]. The MicroAHRS digitizes at a sample rate that is user selected between 1 and 100 Hz, and 16-bits of dynamic bandwidth. Raw

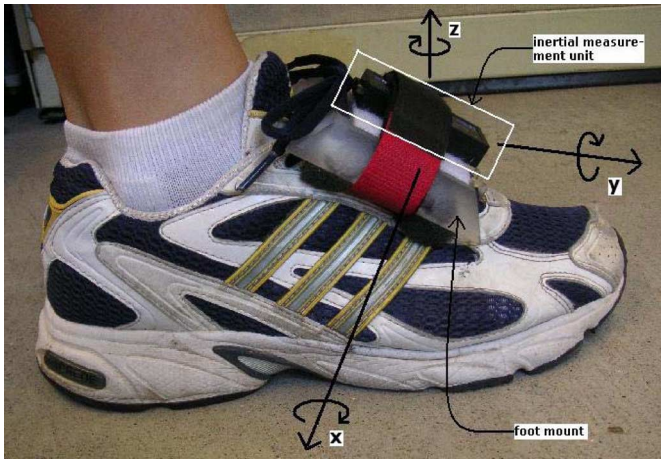

Fig. 1. Diagram of sensor orientation on the shoe.

and corrected data are transmitted by the Bluetooth wireless communication protocol to a nearby handheld personal digital assistant (PDA, Nokia N810). Fig. 1 shows the sensor orientation on the subject's shoe and the corresponding directions of the x, y, and z axes for acceleration, rotation, and heading that are used in this paper. The inertial unit is mounted on the shoe with the foam-padded polymethylmethacrylate (PMMA) plastic foot mount with holes to thread shoelaces through. This apparatus allows the sensor to be tied down tightly, reducing the "sensor jolting" documented by others [12] and ensuring that the data accurately reflect the movement of the underlying foot rather than movement between the sensor and foot.

B. Test to Validate Gyroscope Algorithms

The gyroscope outputs data as an angle rate, in radians per second. It is easier to understand foot motion in the physically relevant measures of degrees rotated in the three orthogonal directions. To obtain this, the angle rate needed to be integrated over time to produce the angle swept during a certain time period. The trapezoidal rule of integration was used, with subintervals of integration equal to the inverse of the sensor sampling rate ($\Delta t = 10$ ms).

Rotation is used to create transformation matrices that are used to transfer the coordinate system from the body frame, a moving coordinate system of the sensor and the shoe, to an inertial frame, a fixed reference to the ground [20]. The transformation matrix from the body to the inertial frame, for rotation about the x axis is

$$X^{-1} = \begin{bmatrix} 1 & 0 & 0 \\ 0 & \cos\theta_x & -\sin\theta_x \\ 0 & \sin\theta_x & \cos\theta_x \end{bmatrix}. \tag{1}$$

The transformation matrix for rotation about the y axis is

$$Y^{-1} = \begin{bmatrix} \cos\theta_y & 0 & \sin\theta_y \\ 0 & 1 & 0 \\ -\sin\theta_y & 0 & \cos\theta_y \end{bmatrix}. \tag{2}$$

And the transformation matrix for rotation about the z axis is:

$$Z^{-1} = \begin{bmatrix} \cos\theta_z & -\sin\theta_z & 0 \\ \sin\theta_z & \cos\theta_z & 0 \\ 0 & 0 & 1 \end{bmatrix}. \tag{3}$$

To transfer the coordinates in a 3-D space, these three matrices need to be multiplied together. In doing so, the order of rotation matters as rotation, i.e., multiplication, is not commutative and multiplying the transformation matrices in different orders produces different results. For example, an order of transformation defined by $[Z^{-1}Y^{-1}X^{-1}]$ produces a transformation matrix, shown in (4), at the bottom of this page.

However, a different order of transformation would produce a different transformation matrix. As a result, for large angles, a unique solution to the problem cannot be obtained. However, a small angle approximation can be made, such that

$$\begin{aligned} \cos d\theta &\cong 1 \\ \sin d\theta &\cong d\theta \\ d\theta \times d\theta &\cong 0. \end{aligned} \tag{5}$$

This is a valid approximation in our application because we are integrating small changes in angle over small time steps of 1/100 seconds. Applying this approximation, the 3-D transformation matrix becomes

$$Z^{-1}Y^{-1}X^{-1} \cong \begin{bmatrix} 1 & -d\theta_z & d\theta_y \\ d\theta_z & 1 & -d\theta_x \\ -d\theta_y & d\theta_x & 1 \end{bmatrix} \tag{6}$$

where dθ denotes the angle between the body frame and the inertial frame. Any order of multiplying the transformation matrices results in this 3×3 transformation matrix, producing a unique solution to the problem. While total angles covered during a step may be large, the integration occurs between individual samples. With the high sampling rate of 100 Hz, and corresponding small time steps for integration of 1/100 seconds, then, small-angle approximation is valid. The changes in angle between when the matrices are multiplied are small, and integration of the gyroscope rate gives accurate results of the angle covered.

To remove sensor drift in the analysis of data from accelerometers, there is a technique known as "zero velocity updating," which assesses the accelerometer drift with every step to remove the cumulative effects [21]. In our gyroscope algorithms,

$$Z^{-1}Y^{-1}X^{-1} = \begin{bmatrix} \cos\theta_y\cos\theta_z & -\cos\theta_x\sin\theta_z + \sin\theta_x\sin\theta_y\cos\theta_z & \sin\theta_x\sin\theta_z + \cos\theta_x\sin\theta_y\cos\theta_z \\ \cos\theta_y\sin\theta_z & \cos\theta_x\cos\theta_z + \sin\theta_x\sin\theta_y\sin\theta_z & -\sin\theta_x\cos\theta_z + \cos\theta_x\sin\theta_y\sin\theta_z \\ -\sin\theta_y & \sin\theta_x\cos\theta_y & \cos\theta_x\cos\theta_y \end{bmatrix}. \tag{4}$$

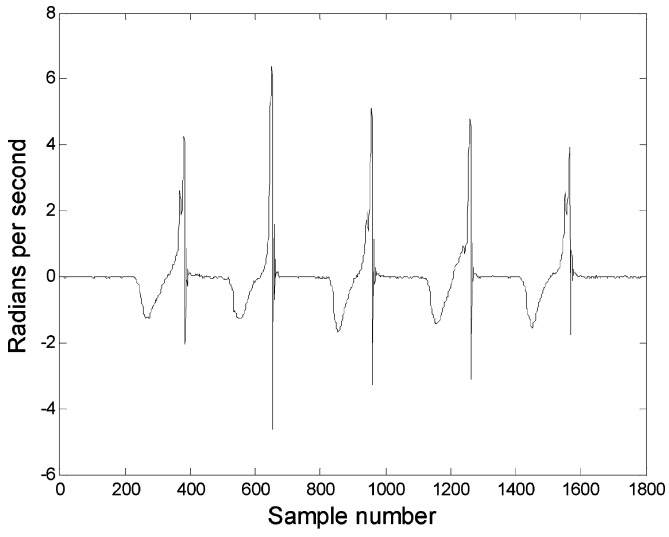

(a)

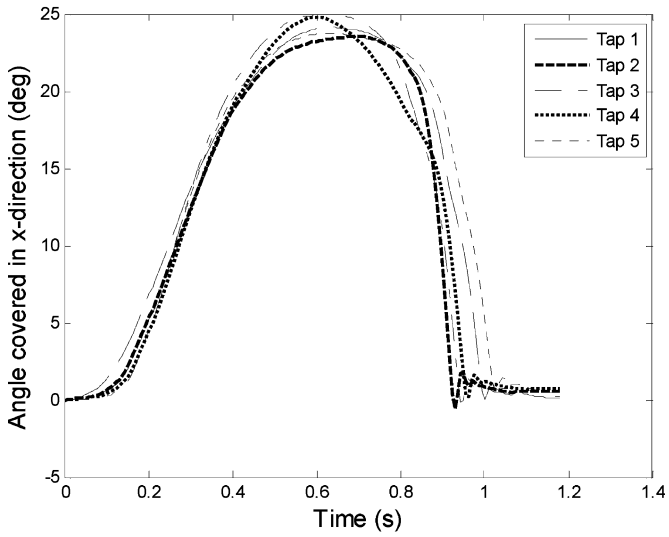

(b)

Fig. 2. (a) Raw x-direction gyroscope data for tapping foot test. (b) Result of applying gyroscope integration algorithms to raw x-direction data.

a similar technique was applied to remove the effects of sensor drift so that an accurate integration results.

A test was performed to ensure that the sensors' gyroscopes output accurate and reliable data, and to validate the preciseness of the gyroscope integration algorithms. The sensor was attached to the foot, and a basic foot motion of tapping while keeping the heel on the ground was performed. This simpler analysis, with motion consisting mostly of a rotation in the x-direction and with minimal translational components, was done before examining the complicated movement of taking a step as part of walking.

Given the nature of the motion, applying the gyroscope integration algorithms to the x-axis raw data produced the most physically relevant result. Fig. 2(a) shows the raw gyroscope data, and Fig. 2(b) is the result of integration for each segmented tap. The segmentation of the data into individual taps is based on the criterion of whether the foot is moving or at rest, i.e., zero velocity. Each line represents one tap of the right foot. Five taps were performed in sequence, with the integration starting at zero each time. While there are slight variations in the movement the foot followed to perform each tap, the overall motion is consistent, as expected, with a maximum angle covered in the x-direction of close to 25°—the actual physical motion of the foot. The sensitivity of the gyroscope sensors and their ability to detect movements within a small error range of ± 0.2 deg/s is observed in the slight oscillations seen at the end of each tap, presumably the vibrations traveling from the ground through the foot to the sensor that result from the impact of the foot hitting the ground.

This validation test shows that the system produces reliable and well-segmented data, which can then be accurately transformed into absolute rotation. Analysis provides numerical measures of rotation that are easily visualized and are analogs of the actual physical motions. These values of 3-D angular displacement and attitude are the physical measures clinicians utilize subliminally in evaluating the gait of patients with suspected neurological disease.

C. Preliminary Experiments to Validate Acceleration-to-Displacement Algorithms

Most people cannot easily visualize or understand the physical meanings of an acceleration time history. Instead, displacement is the measure that allows clinicians to understand and visualize the movements of a patient. A simple double-integration of acceleration to obtain accurate values of displacement for a data segment of even just a few seconds long is difficult [12], given noise recursion, accelerometer drift, and the effect of gravity, which is orientation-dependent, on the raw values of acceleration. There is a solution, however, to these issues. The technique of "zero velocity updating" (zupting), which assesses the drift of the accelerometer with every step, and thus allows the removal of the effects of drift over one step, produces accurate displacement values after double integration [21]. The individual steps are then combined, one after the other, to provide a time history of the body's movement through time, e.g., taking a walk.

In our system, the raw accelerometer data are transformed from the Lagrangian to an inertial frame and 3-D position as a function of time using a proprietary method provided by a colleague. This process is described in detail in the referenced patient [20]. Application of this algorithm results in very accurate 3-D absolute displacement and absolute heading from which to perform our analyses. The horizontal error rates from using the algorithms as described in [22] are on the order of 0.5% of the distance traveled for walks less than 500 m and below 2% for walks up to 8000 m. The vertical error rates are not dependent on the distance traveled and are on the order of 0.75% of the distance traveled. Fig. 3(a) shows the raw accelerometer data in the x-, y-, and z-directions, and Fig. 3(b) shows the resulting displacement values in the inertial frame for five steps. The figures present an enhanced understanding of the walking motion of the foot, providing repeatable continuous displacement

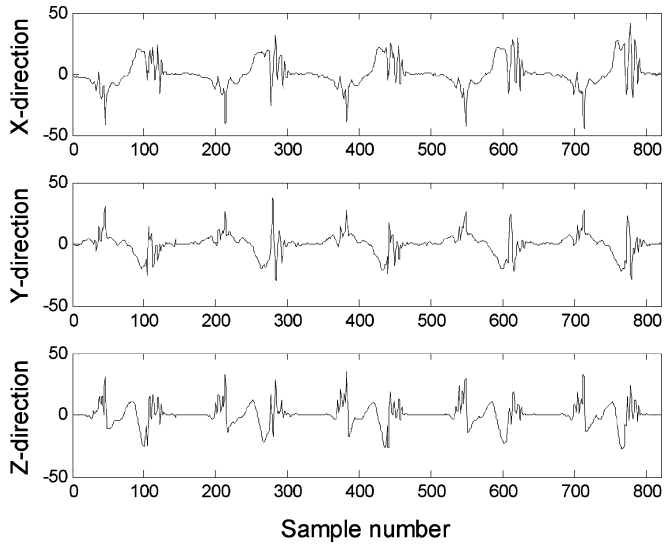

(a)

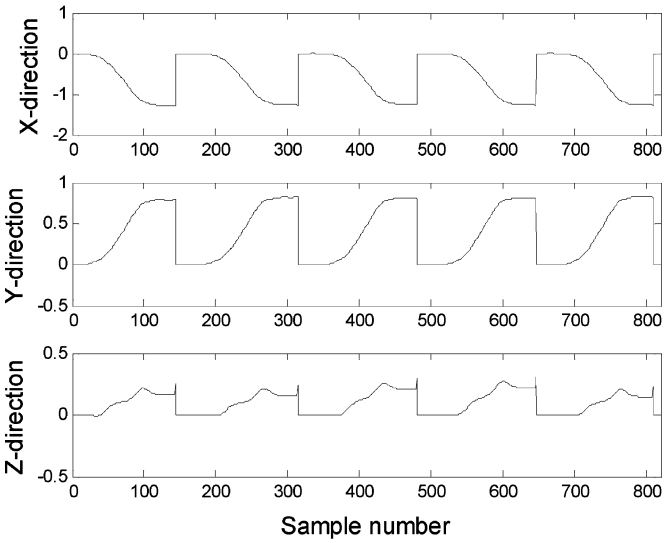

(b)

Fig. 3. (a) Raw three-axis accelerometer data (m/s^2) for five steps of walking. (b) Three-axis displacement output (m) from accelerometer data.

measurements during each step, a hitherto unappreciated measure of gait.

A set of preliminary experiments that allow examination of the better-known numerical gait parameters of cadence and stride length was performed. Two members of the research team, one young 19-year-old woman and one elderly 70-year-old woman, participated in this initial round of data collection, before the system was used to collect data from the control cohort. They were chosen based on their age disparity, so as to demonstrate the ability of the system to reproduce the results of previous studies examining the effects of age on gait. With a sensor attached to the shoe, both subjects walked along a predesignated path around the UC Berkeley campus, a distance of over 1 km, with each trial taking approximately 20 min. The path included walking indoors and outdoors, uphill and downhill, and up stairs and down stairs. Data were collected in the morning (AM) and afternoon (PM) of the same day for each subject.

TABLE I
RESULTING GAIT METRICS OF THE MEANS AND STANDARD DEVIATIONS (SD) OF CADENCE (STEPS PER MINUTE) AND STRIDE LENGTH (IN METERS) FOR PRELIMINARY GAIT ANALYSIS EXPERIMENTS

Terrain	Subject	Time	Cadence (steps/min)		Stride length (m)	
			Mean	SD	Mean	SD
Uphill	Young	AM	54.8	2.76	1.54	0.03
	Young	PM	51.4	2.11	1.44	0.06
	Aged	AM	56.4	1.60	1.20	0.05
Downhill	Young	AM	59.5	2.54	1.53	0.03
	Young	PM	57.3	2.70	1.36	0.05
	Aged	AM	62.0	1.30	1.19	0.02
Up stairs	Young	AM	54.3	1.01	0.55	0.02
	Young	PM	47.8	1.98	0.65	0.13
	Aged	AM	41.2	2.60	0.69	0.16
Down stairs	Young	AM	70.5	3.25	0.55	0.01
	Young	PM	59.6	3.12	0.57	0.03
	Aged	AM	45.5	1.35	0.56	0.02

Similar to the gyroscope data analysis, the displacement data are first segmented into individual steps based on when the foot comes to rest, i.e., zero velocity, at the end of each step. Knowing the sample rate allows the conversion of the sample number to time, and thus cadence; resolving the x- and y-direction displacement data gives the distance traveled in the horizontal plane of the ground (the xy plane), and thus stride length. Calculating the cadence and stride length for each step allows for statistical analysis of the data. The results are shown in Table I. For each subject, the algorithms compute the mean values of the metrics, allowing for comparison of the metrics between subjects. Recording the age of the subject and the time of day of the data collection allows conclusions to be drawn between the differing metrics and the varying subject characteristics. The statistical analysis also includes calculations of gait variability as expressed through the standard deviation (SD) from the mean for each metric. These numerical parameters allow for an evaluation of an individual subject's stride-to-stride variability, where a high variability may indicate an inability of the subject to maintain a steady gait in changing physical settings or especially challenging terrain. Knowing that there is increased stride-to-stride variability in, for example, patients with Parkinson's disease [1] or multiple sclerosis [4] compared to controls, this capability of the system will be valuable in assessing the presence of such neurological diseases.

Although the data presented in Table I are only for two subjects, a very small cohort, the number of steps over which the measures were calculated are large (including at least 50 full gait cycles each for the uphill and downhill segments and 14 full gait cycles each for the up stairs and down stairs segments), so that there are sufficient trials to make a robust estimate.

While one may expect the stride lengths up stairs to be almost equal due to the constant dimensions of the steps of a staircase, the variations shown in Table I can be explained by noting that only the vertical z-dimension of a step is fixed, while stride length is a measure of horizontal distance covered in the

xy-plane. Thus, our system measures the actual length of the step taken to go up a stair, rather than just the height of the step. If, for example, a subject was fatigued, and needed to take a more roundabout route to navigate a step, such as sweeping an arc around the step instead of bending the knee and using maximum muscle power to take a straight path up a step, this action would be reflected in the stride length results. Comparing the young AM and young PM results shows this to be the case. In addition, taking a roundabout route up a step lends itself to higher variations between steps compared to consistently taking the perpendicular path relative to the step, leading to higher SD values in stride length up stairs as well.

D. Experimental Method for Control Subjects

In order to be able to diagnose various neurological diseases based on features of a patient's gait, discriminant features must be found for any form of pattern recognition. One of our goals is to create a system consisting of physically-based measures that clinicians will be able to understand and visualize in distinguishing between normal and disrupted gait.

To begin building such a system, seven control subjects, males over the age of 50, without history or evidence of neurological disease, were used as a "healthy" cohort. Before the collection of data, subjects provided their age, height, and weight. The inertial measurement units were attached to the shoe using the foam-padded mount, to the wrist using a Velcro elastic wrist support, and to the sternum using a pair of specially designed elastic suspenders. Wearing these sensors, subjects walked along a predetermined path on the UC Berkeley campus. This path included a segment of walking outdoors at a constant pace and slightly downhill, before turning around, walking slightly uphill, and going indoors to walk up stairs, then down stairs.

E. Data Analysis

The data analysis for this cohort utilizes both the gyroscope and accelerometer algorithms that have been validated by the experiments previously described. Current analyses have been focused on the data from the sensor attached to the shoe. Because of the susceptibility of the sensors to drift [21], the data from the gyroscope and accelerometer were segmented separately, based on whether the sensor was moving, to maintain accuracy. The small time differences in each sensor's start-up were accounted for in data alignment to obtain time-aligned segmented sets of data consisting of individual steps.

IV. Initial Control Subject Results

A. 3-D Angular Displacement from Gyroscope Algorithms

With the sensor oriented on the shoe as shown in Fig. 1, the gyroscope algorithms calculate the rotation of the foot, in three directions, for each step in the inertial frame. Data were collected for all seven control subjects along the same predesignated path. As this path consisted of varying terrain, the analysis was performed for separate particular portions of the path. The following results are from the analysis of the outdoors, slightly uphill, portion, consisting of 20–25 full gait cycles for each subject.

As a representative sample of all the subjects, Fig. 4 and Table II show the results from the analysis of one of these subjects, subject A. Fig. 4 presents graphs of the rotation of the foot in the three directions while walking, with each line representing a single step. The bold lines in the graphs indicate the means of the rotations. The same analysis was performed for all seven control subjects, with results presented in Fig. 5 and Table III.

In Fig. 5, each line is the average rotation of the foot around the x-axis for each subject, with the bold line indicating the average rotation over all seven control subjects.

It is insightful to examine the deviation of an individual's data from what is expected for a single control subject, or the control subject mean. Fig. 6 presents the results of two such analyses for foot rotation around the x-axis, with subjects labeled as A and B. The two curves are representative of the two types of deviations from the mean: Subject A is ahead of the mean, while Subject B lags behind the mean. There is an obvious 180° phase mismatch between the two subjects. Subject A is more rapid at the beginning and end of the step cycle, while rotating more slowly during the relatively constant central section of foot flight.

In addition to graphical output, the analyses provide numerical parameters for these rotations as well. For the same subject whose data are depicted in the graphs in Fig. 4, Table II presents numerical values for some of these parameters, including statistical measures of range in terms of the maximum (max) and minimum (min) values of a single parameter, and of variability as expressed through the mean and SD values of particular metrics.

The maximum angle in the x-direction as seen near the beginning of the step indicates the maximum plantarflexion (increasing the angle between the leg and the foot at the ankle) of the foot that occurs between heel contact, through the lifting of the heel, to toe off to initiate a step. The minimum angle in the x-direction reached around two-thirds through the step indicates the maximum dorsiflexion (decreasing the angle between the leg and the foot at the ankle) of the foot when the foot is moving through the air during the swing phase of the step. The numerical values of the maximum and minimum angles reached in the y- and z-directions indicate how much the foot rotates in the two directions over a step. Greater variability in y-direction rotation may be indicative of lateral instability of the foot during walking, whereas large changes in the z-angle can be related to circumduction.

Table III presents numerical values for some of the x-direction foot rotation parameters, as based on Fig. 5. Given are the average values for each control subject, as well as the mean and SD values over all seven control subjects.

B. 3-D Absolute Displacement from Accelerometer Algorithms

The analysis algorithms also provide a much more sophisticated analysis of the movement of the foot during the walk. The continuous 3-D absolute displacement data in the inertial frame

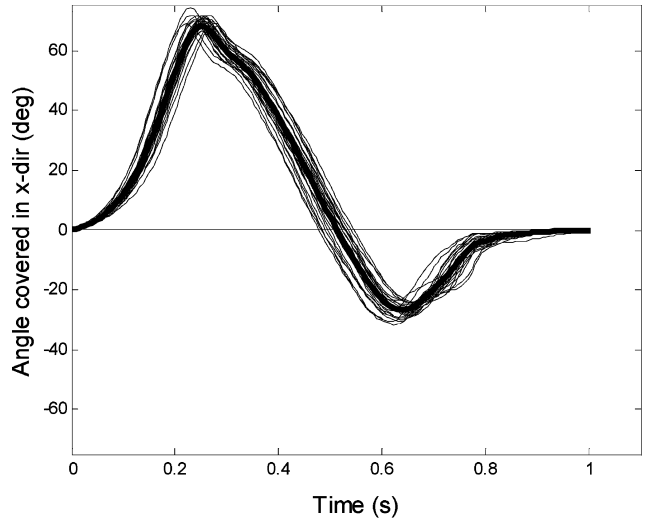

(a)

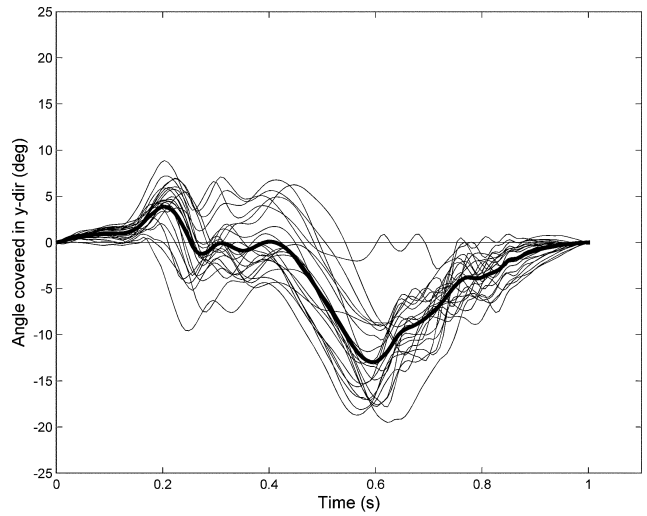

(b)

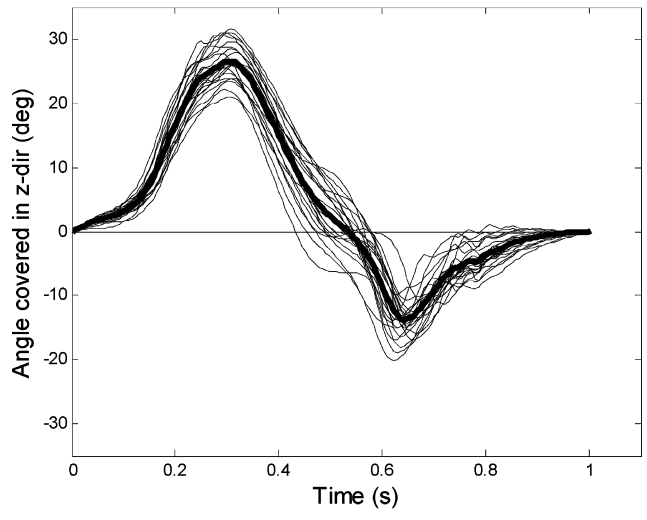

(c)

Fig. 4. (a) Rotation of the foot around the x-axis for each step over the walk for control subject A, compared to the mean over all steps (bold line). (b) Rotation of the foot around the y-axis for each step for control subject A, compared to the mean over all steps (bold line). (c) Rotation of the foot around the z-axis for each step for control subject A, compared to the mean over all steps (bold line).

TABLE II
METRICS FOR FOOT ROTATIONS FOR CONTROL SUBJECT A, WITH ANGULAR DISPLACEMENT VALUES GIVEN IN DEGREES AND TIME IN SECONDS

Maximum angle in x-direction (deg)					
Max	Min	Mean	SD	Time to max (s)	Time as % of total step time
74.2	66.5	70.0	1.94	0.229	24.8
Minimum angle in x-direction (deg)					
Max	Min	Mean	SD	Time to min (s)	Time as % of total step time
-23.6	-31.6	-27.6	2.49	0.623	66.4
Maximum angle in y-direction (deg)					
Max	Min	Mean	SD	Time to min (s)	Time as % of total step time
8.9	0.5	4.8	2.24	0.203	21.7
Minimum angle in y-direction (deg)					
Max	Min	Mean	SD	Time to min (s)	Time as % of total step time
-2.9	-19.5	-13.9	4.12	0.623	62.1
Maximum angle in z-direction (deg)					
Max	Min	Mean	SD	Time to min (s)	Time as % of total step time
31.5	21.0	26.8	2.95	0.308	31.6
Minimum angle in z-direction (deg)					
Max	Min	Mean	SD	Time to min (s)	Time as % of total step time
-9.9	-20.2	-14.7	2.56	0.623	64.6

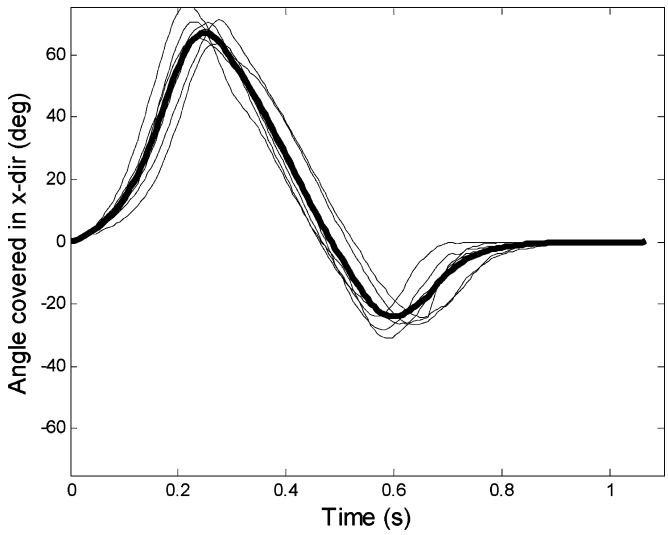

Fig. 5. Average rotation of the foot around the x-axis for each control subject. The mean is indicated by the bold line.

TABLE III
METRICS FOR x-DIRECTION FOOT ROTATIONS FOR ALL CONTROL SUBJECTS

Subject	Maximum angle (deg)	Minimum angle (deg)
A	70.0	-27.6
B	72.0	-24.1
C	67.1	-27.7
D	72.1	-24.9
E	70.5	-30.6
F	77.3	-25.2
G	70.6	-31.5
Mean	71.4	-27.4
SD	3.1	2.9

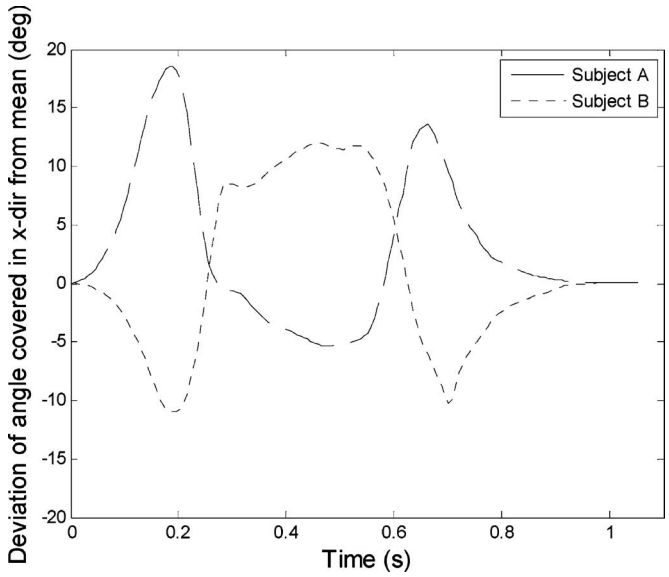

Fig. 6. Deviation from control subject mean of foot rotation around x-axis for two subjects A and B.

allow reconstruction of the total path traveled by the subject and of specific foot movements over time, both in the horizontal xy-plane of the ground as expressed by the distance traveled, and in the vertical z-direction. Again, this analysis was carried out for all seven control subjects, and for the same particular portion of the path. Fig. 7 shows, as a representative sample, one of these analyses that was performed for the same control subject A as in Fig. 4. In the graphs, each line represents a single step, and the means of the displacements are indicated by the bold lines.

Fig. 7(a) shows the horizontal distance traveled in the xy-plane of the ground for each step. As the subjects did not walk in a straight line, but followed the curve of the path, the distance is calculated by resolving the x- and y-direction displacement values. The maximum distance reached for a particular step is the stride length for that step. Fig. 7(b) is the plot of the displacement of the foot in the vertical z-direction for each step.

In Fig. 8, each line represents the average rotation distance traveled in the horizontal xy-plane of the ground for each subject, with the bold line indicating the average distance traveled over all seven control subjects.

Similar to Fig. 6, it is productive to look at the deviation of an individual's data from what is expected for a control subject, or the control subject mean. Fig. 9 presents the results of the analyses for distance traveled in the xy-plane for the same two subjects as in Fig. 6, labeled as Subjects A and B. The two curves are representative of the two types of deviations from the mean, with Subject A once again ahead of the mean, and Subject B lagging behind the mean.

Similar to the gyroscope algorithms, the displacement algorithms provide detailed numerical parameters. For the same subject whose data are depicted in Fig. 7, Table IV provides some important gait parameters, including statistical measures of range in terms of the maximum (max) and minimum (min) values of a single parameter, and of variability as expressed through the mean and SD values of particular metrics.

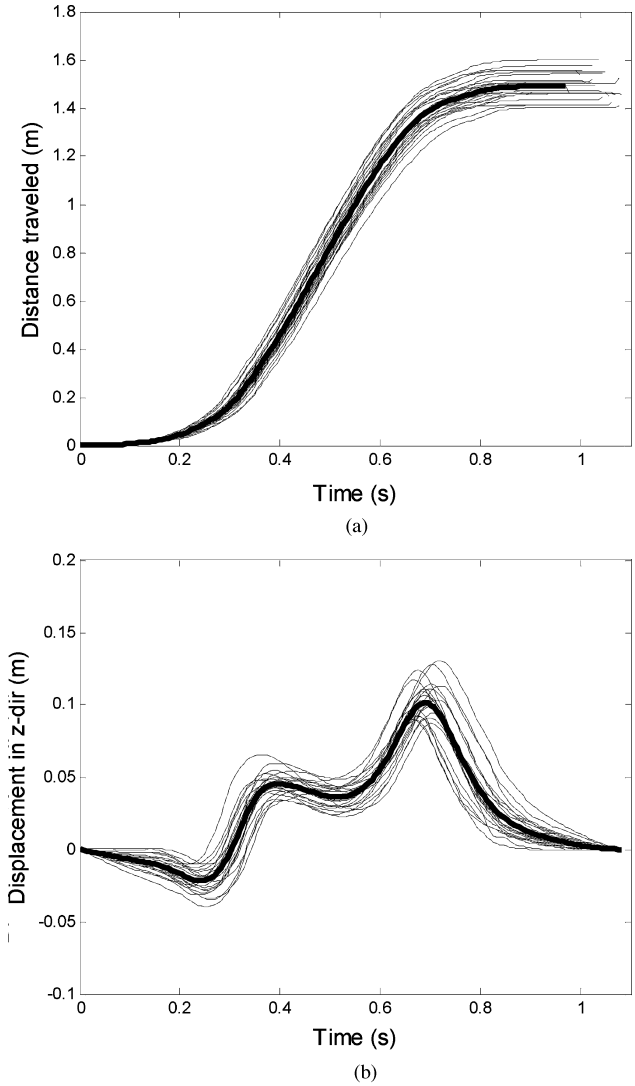

Fig. 7. (a) Distance traveled in the xy- plane for each step over the walk for control subject A, compared to the mean over all steps. (b) Displacement of the foot in the z-direction for each step for subject A, compared to the mean over all steps.

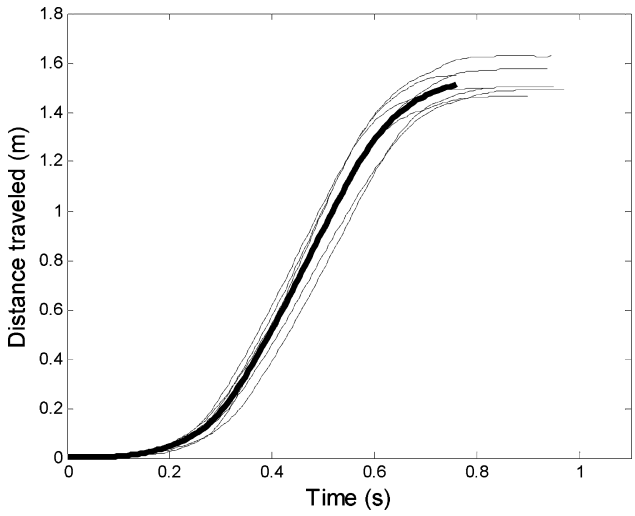

Fig. 8. Average distance traveled in the xy-plane for each control subject.

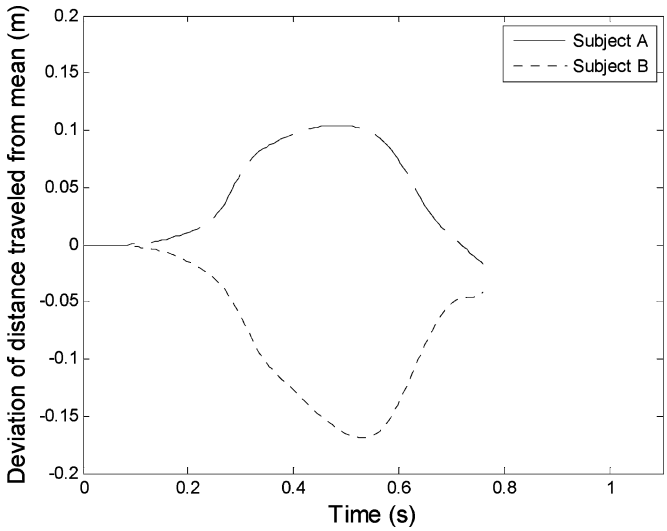

Fig. 9. Deviation from control subject mean of distance traveled in the xy-plane for two subjects A and B.

TABLE IV
METRICS FOR THE DISPLACEMENTS OF CONTROL SUBJECT A, WITH DISPLACEMENT VALUES GIVEN IN METERS AND TIME IN SECONDS

Maximum displacement in vertical z-direction (m)					
Max	Min	Mean	SD	Average time to max (s)	Time as % of total step time
0.130	0.087	0.105	0.013	0.721	67.5
Cadence (steps/min)					
Max		Min		Mean	SD
55.5		48.7		50.7	1.630
Stride length (m)					
Max		Min		Mean	SD
1.60		1.41		1.49	0.053
Velocity (m/s)					
Max		Min		Mean	SD
1.39		1.16		1.26	0.071
% of step that foot is moving (vs. stationary)					
Max		Min		Mean	SD
86.7		77.1		82.0	1.775

The maximum displacement in the vertical z-direction is the maximum rise of the foot as it moves through the air during the swing phase of a step. Cadence (steps per minute) gives the frequency of steps, while stride length gives the distance covered in a single step. Looking at a full gait cycle, velocity combines both the cadence and stride length variables into an overall measure of how fast the subject is moving while walking. Breaking down a step into a percentage of time when the foot is moving compared to when it is stationary shows how long the subject is in the swing phase compared to the stance phase of a step.

Table V presents numerical values for some of the parameters of displacement in the xy-plane, as based on Fig. 8. Given are the average values for each control subject, as well as the mean and SD over all seven control subjects.

C. Physically-Based Model of the Foot for Visualization

Combining the gyroscope and displacement algorithms gives the rotational and translational components necessary to fully describe the motion of the foot as it moves through the air for each step. Our algorithms use this information to allow visualization of the foot while walking. Using an ellipsoid as a model of the foot, Fig. 10 shows, top and bottom, still shots from a video of a foot while walking and the corresponding stills from the animation of the ellipsoid based on the analyzed data.

TABLE V
METRICS FOR DISPLACEMENT IN THE xy-PLANE FOR ALL CONTROL SUBJECTS

Subject	Cadence (steps/min)	Stride length (m)	Velocity (m/s)
A	50.7	1.49	1.26
B	52.7	1.47	1.29
C	49.3	1.58	1.29
D	54.6	1.50	1.37
E	62.6	1.55	1.62
F	56.6	1.50	1.41
G	54.1	1.63	1.47
Mean	54.4	1.53	1.39
SD	4.4	0.06	0.13

Fig. 10. Still shots from a video of a foot while walking and the corresponding animation output by our algorithms to create a model for visualization.

V. DISCUSSION

The data presented here have shown that the increased granularity of measurements of gait motions makes a more physical interpretation of walking motions possible. Analysis of Table I from the preliminary experiments shows that the young subject had a higher cadence and longer stride length in the morning than afternoon in the uphill and downhill segments, perhaps the result of fatigue of the subject through the course of the day. The decreased cadence between morning and afternoon is especially pronounced for the young subject when walking down stairs. In walking up and down stairs, the elderly subject had a lower cadence compared to the young subject, as stairs are a more difficult and complex terrain for the aged to navigate. In walking uphill and downhill, the elderly subject had a higher cadence and shorter stride length than the young subject, a finding consistent with previous studies of the effect of aging on gait [23]. With higher SD values, the elderly subject displayed greater variability than the young subject in both cadence and stride length when walking up stairs. Studies have postulated that increased variability in gait among the elderly is the result of decreased strength and flexibility [24]. As walking up stairs requires a significant amount of strength to lift the mass of the body up the height of a step and flexibility to lift the leg up the height of a step, the increased variability shown in Table I for the elderly subject is consistent with past results. Due to the physical challenge of walking up stairs, it is probable that, unlike walking along smooth slopes, a subject's gait metrics are

determined in large part by balance-control mechanisms as opposed to the gait-patterning mechanism. It has been found that the gait variables determined by balance-control mechanisms have increased variability with age [23], a result shown here. The consistency of the experimental results with previous work provides validation for the accuracy of both the initial conversion of acceleration to displacement, and the subsequent analysis of the displacement data.

From the control subject experiments, for a given individual, the graphs of rotation of the foot in three orthogonal directions (see Fig. 4) show consistency in both shape and amplitude across many steps. People are quite constant in their gait from step to step, and therefore analyses of the subtleties on an individuals' gait can be made. The y-rotation graph [see Fig. 4(b)] shows the most variation among the 6-DOF measurements. The amplitudes of the motions are relatively small but significant because the degree of pronation of the foot is a strong indicator between subjects, for example, it is an important parameter for choosing running shoes. The three graphs allow for a straightforward understanding of the flight motion of the foot through the air for each step. The aligned zero-points for the rotations around the x-axis [see Fig. 4(a)] and z-axis [see Fig. 4(c)] show that the transition from plantarflexion of the foot to dorsiflexion (x-axis rotation) occurs simultaneously as the transition from a clockwise rotation from center to counterclockwise (z-axis rotation), a fact not distinguishable by the naked eye.

The graphs of foot displacement (see Fig. 7) provide much more detailed spatiotemporal information for the walking foot than the cadence and stride length examined in previous studies. The displacement graphs show consistency in both shape and amplitude for a single subject across steps for the walking motion, both in the xy-plane of the ground in terms of distance traveled [see Fig. 7(a)] and in the z-direction displacement [see Fig. 7(b)].

The graphs of rotation of the foot around the x-axis (see Fig. 5) and of distance traveled in the horizontal xy-plane of the ground (see Fig. 8) for each subject show consistency in the overall motion for all control subjects, with only slight variation between individual subjects. Taking the mean to obtain these results introduces some artifacts, such as the rounding of the peak in Fig. 5. However, we are looking at the overall shapes of the curves, and thus these artifacts are relatively insignificant. In addition, the averaging is necessary to establish a model for the healthy cohort. The consistency for the healthy cohort shown in Figs. 5 and 8, along with the data to be collected from patients with neurological disease, will allow the two groups to be distinguished.

The numerical parameters obtained by the gyroscope algorithms (Table II) are medically relevant variables as found in previous studies on neurological disease. A smaller magnitude of the minimum angle reached in the x-direction shows decreased dorsiflexion, which is an indicator of foot drop. In multiple sclerosis, foot drop has been shown to be due to decreased muscle endurance of the legs and reduced dorsiflexor control during walking [25]. While the magnitudes of the maximum and minimum angles in the y-direction are the smallest of the three coordinates, they display the highest SD values. Greater variability in these y-angle parameters coordinates with instability of the foot, an inability to keep the foot level to the ground, and reduced muscle strength in the ankle, during the motion of taking a step. Such muscle weakness in the ankle has been found to be one of the causes for postural instability in patients with Parkinson's disease [26]. Greater magnitudes of the maximum and minimum angles in the z-direction, or larger differences between the high and low extremes of z-direction rotation of the foot during a step, are a way to measure foot circumduction, a known feature of certain gait disorders [27].

Comparison of Figs. 6 and 9 provides insight into how an individual's motion deviates from the motion expected for a control subject, as determined by the mean calculated over all control subjects. Subject A is ahead of the mean for both foot rotation around the x-axis (see Fig. 6) and distance traveled in the xy-plane (see Fig. 9). These two deviations are related in that because he reaches his maximum angle in the x-direction sooner, as evidenced by the peak at the beginning of the step in Fig. 6, he is able to initiate the swing phase of his step sooner, and cover the distance of the step sooner, as evidenced by the positive deviation from the control subject mean in Fig. 9. This physical explanation also accounts for the negative deviation in the middle of the step for the rotation around the x-axis. Since Subject A reached his maximum x-angle earlier, he is also ahead of the mean during the dorsiflexion of the foot, with a foot angle less than the mean during this phase of the step. Conversely, Subject B lags behind the mean in both measures. It takes him longer to reach his maximum angle in the x-direction, so it is later when he begins the swing phase of his step, leaving him below the mean for distance traveled for the duration of the step. The positive deviation seen in Fig. 6 for foot rotation around the x-axis during the middle of the step is due to a later beginning of the dorsiflexion phase of the step compared to the mean.

A thorough literature review has shown that these rotation parameters of gait have not been studied previously. Thus, no published reference data are available with which to compare our results for validation. Gait analysis has consistently focused on cadence, stride length, and velocity. As clinicians take into account a much broader range of gait characteristics when evaluating patients, this shows the importance of the new science of our system in providing quantified measurements of these gait parameters as well, including rotation.

The metrics obtained from the displacement algorithms (Table IV) are medically relevant variables used in the evaluation of gait. A larger magnitude of the maximum vertical z-direction displacement of a foot during the swing phase of a step is indicative of steppage gait, which occurs in a variety of neurological disorders. The common metrics of cadence and stride length have been studied widely in previous work on gait disruptions in patients with neurological disease [2]; patients with multiple sclerosis, for example, walk with reduced cadence and stride length [9]. Velocity is a variable of gait that has been found to be influenced strongly by the onset of disease [27]. Measuring the percentage of time during walking that the foot is moving or stationary gives a measure of gait cycle timing. Variability in this timing correlates with severity of Parkinson's disease [1].

The results tabulated in Table V are consistent with previous studies of gait. The control subject means for stride length and velocity fall within the range found for controls using an alternate method of force-sensitive insoles [28], providing validation for our system. However, force-sensitive insoles are unable to provide information on the flight of the foot between when the foot leaves the ground and when the foot hits the ground again. Similar to the case for rotation parameters, then, there is no previous published data with which to validate the vertical z-direction displacement measurements obtained using our system, as presented in Table IV.

The visualization models (see Fig. 10) allow clinicians to see the slight movements of the foot while walking that might otherwise not be apparent. For example, instead of giving a fixed point in time when the foot hits the ground, the algorithms produce an animation over time of how exactly the foot moves as it makes contact with the ground. The models can be scaled to slow down or speed up motions in order to focus on particular relevant portions of a step, such as how the foot makes contact with the ground. These details, which are what clinicians currently observe, are important in distinguishing between patients and healthy controls. Our system is able to visualize and quantify these minutiae.

VI. Conclusion and Future Work

The control subject results presented in this paper illustrate the ability of our sensor and algorithms system to provide a detailed quantitative understanding of the movement of the foot while walking, an improvement over existing gait analysis systems. What is new and important in this paper is a presentation of the 6-DOF (3-D angular displacement and 3-D absolute displacement) analysis from our system. The results of the differences found between young and aged subjects, and between data taken in the morning and afternoon, are supported by existing gait literature. The results from our set of control subjects quantify features of gait currently used by clinicians to diagnose and evaluate neurological disease. The analysis was done both for single subjects to determine the values of gait parameters specific to an individual, and over the cohort to develop a control set of data with which diseased patients can be compared.

In the next step in our investigations, we can begin to decide whether this system can be used to enhance the subjective judgments made by clinicians in evaluating patients. We are working on integrating the data from the wrist and sternum sensors into the analyses of the foot sensor data currently collected. A challenge in doing so is aligning the data in space and time from the different sensors to create a synchronized model.

Another challenge is in segmentation of the wrist and sternum sensor data, because while the foot comes to a stop every step while walking, which allows for straightforward segmentation based on whether the sensor is moving, the arm and upper body have an additional rigid-body velocity (drift in the data) that rapidly becomes overpowering through integration. Thus, the zupting technique cannot be directly utilized in the segmentation of the wrist and sternum sensor datasets. We are investigating segmentation within a moving reference frame relative to the center of gravity (COG), and the COG relative to the foot, which will allow for analysis of the position and movement of the arm and torso relative to the feet during walking.

Two variables of gait that may pose a challenge to analysis are the width of the base (distance between feet) during walking and how a patient holds the arms. These variables require us to be able to ascertain the position of the sensors relative to each other. A possible solution to this issue is to have subjects start an experiment with their arms to their sides and feet together. Then, the data from consequent motions will give the numerical measures of a subject's natural position while walking.

An additional application for our system is in physical activity monitoring. We are currently working to obtain numerical data on boys with Duchenne muscular dystrophy so as to characterize features such as the amount of mobile versus sedentary behavior; the degree of activity, such as running versus walking; and the type of activity, including indoors versus outdoors activity. These characterizations may provide numerical measures of drug efficacy in improving quality of life.

As we collect data from control subjects in order to perform pattern recognition, data from patients with neurological disease are required to distinguish between healthy and ill. Examining both sets of data will lead to further robustness of feature extraction. An advantage of our algorithms is that they are fully automated to minimize the effort needed to perform many tests. The analyses that have been performed so far, and that have been described in this paper, show our system to be a viable way forward in attempting to quantify gait. We will continue to develop the system by acquiring more data, analyzing it further, and refining our algorithms.

Acknowledgment

The authors thank L. Hutchings for his contributions to this project.

References

[1] J. M. Hausdorff, M. E. Cudkowicz, R. Firtion, J. Y. Wei, and A. L. Goldberger, "Gait variability and basal ganglia disorders: Stride-to-stride variations of gait cycle timing in Parkinson's disease and Huntington's disease," *Movement Disord.*, vol. 13, no. 3, pp. 428–437, May 1998.

[2] M. E. Morris, R. Iansek, T. A. Matyas, and J. J. Summers, "The pathogenesis of gait hypokinesia in Parkinson's disease," *Brain*, vol. 117, no. 5, pp. 1169–1181, 1994.

[3] M. E. Morris, R. Iansek, T. A. Matyas, and J. J. Summers, "Stride length regulation in Parkinson's disease: Normalization strategies and underlying mechanisms," *Brain*, vol. 119, no. 2, pp. 551–568, 1996.

[4] M. E. Morris, C. Cantwell, L. Vowels, and K. Dodd, "Changes in gait and fatigue from morning to afternoon in people with multiple sclerosis," *J. Neurol. Neurosurg. Psychiatry*, vol. 72, no. 3, pp. 361–365, 2005.

[5] P. Thoumie, D. Lamotte, S. Cantalloube, M. Faucher, and G. Amarenco, "Motor determinants of gait in 100 ambulatory patients with multiple sclerosis," *Multiple Sclerosis*, vol. 11, no. 4, pp. 485–491, 2005.

[6] A. Peppe, C. Chiavalon, P. Pasqualetti, D. Crovato, and C. Caltagirone, "Does gait analysis quantify motor rehabilitation efficacy in Parkinson's disease patients?" *Gait Posture*, vol. 26, no. 3, pp. 452–462, 2007.

[7] L. Middleton, A. A. Buss, A. Bazin, and M. S. Nixon, "A floor sensor system for gait recognition," in *Proc. 4th IEEE Workshop Autom. Identification Adv. Technol.*, 2005, pp. 171–176.

[8] T. Liikavainio, T. Bragge, M. Hakkarainen, J. Jervelin, P. Karjalainen, and J. Arokoski, "Reproducibility of loading measurements with skin-mounted accelerometers during walking," *Arch. Phys. Med. Rehabil.*, vol. 88, no. 7, pp. 907–915, Jul. 2007.

[9] M. G. Benedetti, R. Piperno, L. Simoncini, P. Bonato, A. Tonini, and S. Giannini, "Gait abnormalities in minimally impaired multiple sclerosis patients," *Multiple Sclerosis*, vol. 5, no. 5, pp. 363–368, 1999.
[10] S. J. Morris and J. A. Paradiso, "A compact wearable sensor package for clinical gait monitoring," *Offspring*, vol. 1, no. 1, pp. 7–15, Jan. 2003.
[11] S. J. Morris, "A shoe-integrated sensor system for wireless gait analysis and real-time therapeutic feedback," Doctoral thesis, Massachusetts Inst. Technol., Cambridge, MA, Jun. 2004.
[12] A. M. Sabatini, C. Martelloni, S. Scapellato, and F. Cavallo, "Assessment of walking features from foot inertial sensing," *IEEE Trans. Biomed. Eng.*, vol. 52, no. 3, pp. 486–494, Mar. 2005.
[13] B. Auvinet, G. Berrut, C. Touzard, L. Moutel, N. Collet, D. Chaleil, and E. Barrey, "Reference data for normal subjects obtained with an accelerometric device," *Gait Posture*, vol. 16, no. 2, pp. 124–134, Oct. 2002.
[14] J. J. Kavanagh, S. Morrison, D. A. James, and R. Barrett, "Reliability of segmental accelerations measured using a new wireless gait analysis system," *J. Biomech.*, vol. 39, no. 15, pp. 2863–2872, 2006.
[15] S. Lord, L. Rochester, K. Baker, and A. Nieuwboer, "Concurrent validity of accelerometry to measure gait in Parkinson's disease," *Gait Posture*, vol. 27, no. 2, pp. 357–359, Feb. 2008.
[16] I. P. Pappas, M. R. Popovic, T. Keller, V. Dietz, and M. Morari, "A reliable gait phase detection system," *IEEE Trans. Neural Syst. Rehabil. Eng.*, vol. 9, no. 2, pp. 113–125, Jun. 2001.
[17] W. Zijlstra, "Assessment of spatio-temporal parameters during unconstrained walking," *Eur. J. Appl. Physiol.*, vol. 92, no. 1/2, pp. 39–44, Jun. 2004.
[18] MicroStrain. (2007). 3DM-GX2 product datasheet [Online]. Available: http://www.microstrain.com/pdf/3dm-gx2_datasheet_v1.pdf (accessed Jun. 25, 2008).
[19] *Certificate of Calibration and Conformance*. Model name: MicroStrain ISD, model number: 3065-0006, serial number: 1032, firmware version: 116, technician: JTH, MicroStrain. (2008). [Online]. Available: http://www.microstrain.com
[20] L. Hutchings, "Rotational sensor system," U.S. Patent 6 305 221, 2001.
[21] L. Ojeda and J. Borenstein, "Non-GPS navigation with the personal dead-reckoning system," presented at the SPIE Defense Security Conf., Unmanned Syst. Technol. IX, Orlando, FL, Apr. 9–13, 2007.
[22] P. W. Kasameyer, L. Hutchings, M. F. Ellis, and R. Gross, "MEMS-based INS tracking of personnel in a GPS-denied environment," in *Proc. ION GPS/GNSS*, Long Beach, CA, Sep. 13–16, 2005, pp. 949–955.
[23] A. Gabell and U. S. Nayak, "The effect of age on variability in gait," *J. Gerontol.*, vol. 39, no. 6, pp. 662–666, 1984.
[24] H. G. Kang and J. B. Dingwell, "Separating the effects of age and walking speed on gait variability," *Gait Posture*, vol. 27, no. 4, pp. 572–577, May 2008.
[25] J. Mount and S. Dacko, "Effects of dorsiflexor endurance exercises on foot drop secondary to multiple sclerosis: A pilot study," *NeuroRehabilitation*, vol. 21, no. 1, pp. 43–50, 2006.
[26] M. Nallegowda, U. Singh, G. Handa, M. Khanna, S. Wadhwa, S. L. Yadav, G. Kumar, and M. Behari, "Role of sensory output and muscle strength in maintenance of balance, gait, and posture in Parkinson's disease: A pilot study," *Amer. J. Phys. Med. Rehabil.*, vol. 83, no. 12, pp. 898–908, Dec. 2004.
[27] L. Sudarsky, "Geriatrics: Gait disorders in the elderly," *New Engl. J. Med.*, vol. 322, no. 20, pp. 1441–1446, May 1990.
[28] R. Baltadjieva, N. Giladi, L. Gruendlinger, C. Peretz, and J. M. Hausdorff, "Marked alterations in the gait timing and rhythmicity of patients with de novo Parkinson's disease," *Eur. J. Neurosci.*, vol. 24, no. 6, pp. 1815–1820, 2006.

Iris Tien received the B.S. degree in civil engineering in 2007 from the University of California (UC), Berkeley, where she is currently working toward the Ph.D. degree in civil systems engineering.

Since 2007, she has been a Researcher with the Center for Information Technology Research in the Interest of Society (CITRIS), UC. Her current research interests include applying engineering to solve medical problems. She is a recipient of the Chancellor's Fellowship for Graduate Study from UC, Berkeley.

Ms. Tien is a National Science Foundation Graduate Research Fellow.

Steven D. Glaser received the B.A. degree in philosophy from Clark University, Worcester, MA, in 1975, and the B.S., M.S., and Ph.D. degrees in civil engineering from the University of Texas, Austin, in 1984, 1986, and 1990, respectively.

He graduated the apprentice training program of the International Union of Operating Engineers in 1977. He was a journeyman operating engineer/driller in the USA and Iraq for eight years. He was a Fulbright Scholar at the Technion, Israel. Since 1996, he has been a Professor at the University of California, Berkeley, where he is also the Intelligent Infrastructure Theme Leader at the Center for Information Technology Research in the Interest of Society. He is a Faculty Scientist with the Energy Resources Department, Lawrence Berkeley National Laboratory, Berkeley. He is also a Research Associate of Intel Berkeley Laboratory, Berkeley.

Prof. Glaser has been a member of the National Research Council (NRC) Report Committee, and a recipient of a National Science Foundation (NSF) Young Investigator Award. Since 1996, he has been a Research Engineer at the National Institute of Standards and Technology.

Ruzena Bajcsy (M'81–SM'88–F'92) received the Master's and Ph.D. degrees in electrical engineering from Slovak Technical University, Bratislava, Slovakia, in 1957 and 1967, respectively, and the Ph.D. degree in computer science from Stanford University, Stanford, CA, in 1972.

She was a Professor of computer science and engineering at the University of Pennsylvania until 1998. She was the Assistant Director of the Computer Information Science and Engineering (CISE) Directorate, National Science Foundation. In 2004, she became the Director Emeritus at the Center for Information Technology Research in the Interest of Society (CITRIS), University of California (UC), Berkeley, where he is currently a Full-Time Professor of electrical engineering and computer sciences.

Dr. Bajcsy is a member of the National Academy of Engineering, as well as the Institute of Medicine.

Douglas S. Goodin, photograph and biography not available at the time of publication.

Michael J. Aminoff was born in U.K. He received the M.D. and D.Sc. degrees from the University of London, London, U.K.

In 1974, he joined the School of Medicine, University of California, San Francisco (UCSF), San Francisco, where he has been a Professor of neurology since 1982, and is also the Director of the Parkinson's Disease Clinic and Research Center, where he is involved in a number of clinical trials and physiological studies of patients with movement disorders. He is the author or coauthor of more than 200 published medical or scientific articles, as well as the author or editor of about 27 books, many of which have gone into several editions, and of numerous chapters on topics related to neurology.